PCCP

Accepted Manuscript

ROYAL SOCIETY OF CHEMISTRY

www.rsc.org/pccp

Stereochemical Modulation of Emission Behaviour in *E/Z* Isomers of Diphenyldipyrroethene from Aggregation Induced Emission to Crystallization Induced Emission

K. Garg,[a] E. Ganapathi,[a] P. Rajakannu[a] and M. Ravikanth[a] *

Department of Chemistry, Indian institute of Technology Bombay, Powai, Mumbai- 400076

E-mail: kavitachemistry1@gmail.com, ganapathi@chem.iitb.ac.in, rajakannu@chem.iitb.ac.in, ravikanth@chem.iitb.ac.in

Corresponding Author

Prof. Mangalampalli. Ravikanth, Department of Chemistry, Indian institute of Technology Bombay, Powai, Mumbai- 400076

ABSTRACT

Herein, we report synthesis, separation and characterisation of *E*- and *Z*-isomers of dipyrrolyldiphenylethene to study their emission behaviour in aggregation state and solid state. *E*-isomer showed pronounced Aggregation Induced Emission (AIE) whereas *Z*-isomer showed Crystallization Induced Emission (CIE). Present study explains that emission behaviour (AIE/CIE) is dependent on the inter/intra molecular interactions between the molecules. The study also validates that Restriction of Intramolecular Rotation (RIR) is the

main cause of AIE/CIE in olefinic luminogens (TPE type of systems) rather than E/Z isomerisation.

1. Introduction

From last few decades, a lot of attention has been paid in the direction of organic fluorescent materials for the potential applications in optoelectronic devices, sensors and bioimaging.[1–9] The traditionally used fluorophores undergoes aggregation caused quenching (ACQ) which limits its usability in OLEDs.[10–14] In last decade, an opposite and abnormal phenomenon named aggregation-induced emission (AIE) and crystallization-induced emission (CIE) were observed in a series of propeller-shaped non-emissive dyes.[15,16] Compared with traditional organic emitters, AIE luminogens (AIEgens) and CIE luminogens (CIEgens) are burgeoning class of conjugated molecules with propeller-shaped structures.[7,8,17–19] They are weakly or non-luminescent in their dilute solutions, but emit efficiently when aggregated or fabricated into solid films.[7,18,20] This intriguing property enables them to be potentially applied in highly efficient optoelectronic devices, fluorescent sensors, cell imaging, and so on.[21–28] Some chromophores have both AIE and CIE effects, whereas in some cases, the crystals of AIE dyes emit bluer lights in higher efficiencies than their amorphous counterparts.[29–31] For example, the amorphous (4-biphenylyl)phenyldibenzofulvene weakly emits yellow light, whereas its crystalline film emits a 32-fold higher efficiency blue light.[30] Till date there are variety of luminogens with such characteristics and structural diversity have been developed.[32,33]Among the AIE luminogens developed so far, tetraphenylethene (TPE) is unique because of its synthetic accessibility (one-step reaction) and structural tunability.[17,34–36] There are various mechanisms proposed in literature to explain AIE phenomenon. Among those, the *E/Z* Isomerization (*EZ*I)[9] and the Restriction of Intramolecular Rotation (RIR)[10] are more convincing and supported by experimental results and theoretical studies. In TPE molecule, according to *EZ*I hypothesis, in solution phase, the excited states are non-

radiatively annihilated by the *EZ*I process, but this process is restricted in aggregated phase leading to an increase in the photoluminescence (PL) efficiency.[37–39] Since Photo-isomerization of E-Z stilbene and its derivatives is known for emission quenching in the solutions [40–42] and TPE is structurally a stilbene derivative,; E–Z photoisomerisation accounts for the non-emissive nature of its solution. The suppression of the isomerization by aggregate formation may be responsible for the AIE effect of its aggregates, as the photoinduced conformation change has been considered to be a root cause of quenching fluorescence of unrestrained fluorogens in biological systems, such as blue-fluorescent anti- bodies[43] and green fluorescence proteins (GFP).[44,45] It has been already hypothesized that trapping of the stilbene and hydroxybenzylideneimidazolinone chromophores by the ligand-binding pockets of the antibodies and β-barrel of GFP respectively, have suppressed the E–Z isomerization and revived the fluorescence processes.[43–45] This suggests that restriction in EZI process in aggregation could be the cause of AIE/CIE behavior. On the other hand, according to RIR mechanism, in the solution phase, the dynamic intramolecular rotations (IMR) of its multiple phenyl rotors against its ethylene stator serves as relaxation channel for the decay of excited state. Whereas in the aggregated state, restriction in IMR, blocks the non-radiative energy dissipation channels, and populates the non radiative excitons.[7,10,15,19,46–52] A correct mechanistic understanding of the AIE process is still decipherd.

To study the involvement of *EZ*I process, pure *E*- and *Z*-isomers of an olefinic luminogen are required. The commonly used titanium-catalyzed McMurry coupling reaction generally produces *E/Z* mixtures, which are difficult to separate. Recently, Tang *et. al.* have attached bulky groups like phenoxy hexyl azide to the TPE core for easy separation of *E/Z* mixtures.[7] Although, this approach has explained the non-involvement of EZI process in AIE behavior but it is beneficial to use systems, which are devoid of bulky groups, as it generally depends on intra- or intermolecular interactions. Therefore it is desirable to study novel molecules *via*

simple modifications to directly validate the proposed hypothesis. Here, we have used dipyrrolyldiphenylethene (**DPYDPE)** molecule, which is a propeller shaped molecule like TPE, with two phenyl rings replaced by pyrrole rings to study. The **DPYDPE** molecule is synthesized by using traditional titanium-catalyzed McMurry coupling methodology. The presence of intramolecular H-bonding in pyrrole rings facilitates the separation of the *E*- and *Z*-DPYDPE isomers by crystallization technique. The **DPYDPE** molecule showed switching between AIE and CIE behaviour by altering the stereochemistry of the molecule.

2. Results and Discussion

2.1. Synthesis of *E*- and *Z*-isomers of DPYDPE

We have synthesized dipyrrolyldiphenylethene (DPYDPE) from 2-benzoylpyrrole using traditional McMurry coupling in presence of Zn and $TiCl_4$ in THF and isolated the *E/Z* mixture of DPYDPE in 52% yield after neutral alumina column chromatographic purification (**Scheme 1**). We have successfully separated the *E*- and *Z*-isomers from the mixture by fractional crystallization technique. One of the isomer was obtained as yellow crystals by crystallization of *E/Z* mixture from CH_2Cl_2/hexane followed by washing with CH_2Cl_2. On evaporation of washed CH_2Cl_2 layer, followed by slow crystallization from CH_2Cl_2/ hexane furnished another isomer as colorless needles. Both of these isomers were characterized by X-ray crystallography.

2.2. Characterization of *E*- and *Z*-DPYDPE

X-ray crystallography revealed that the yellow crystals were *Z*-DPYDPE whereas colorless needles were *E*-DPYDPE as depicted in **Figure 1** and crystallographic data provided in **Table-1**. The *Z*-isomer crystallized into triclinic space group P-1, whereas as *E*-isomer was found to be in tetragonal space group 41/a. Two carbon atoms of ethene group in *E*-isomer shows a positional disorder with two positions for the ethene group with equal occupancy. Only one of the two occupancies of the ethene group is depicted in Figure **1a**. In *Z*-isomer,

asymmetric unit was composed of single molecule with disordered geometry. Whereas, in *E*-isomer, the asymmetric unit was composed of one half of the molecule, where all the atoms were symmetry-disordered by the two-fold axis The dihedral angles between two phenyl rings and two pyrrole rings were 8.89^{o} and 6.44^{o} for *Z*-isomer respectively, whereas the respective angles for *E*-isomer were 176.19^{o} and 179.22^{o}. Z-DPYDPE also showed intramolecular H-bonding, where only one pyrrole NH was involved in H-bonding with a bond angle (N1-H1W---N2) of 104.16^{o}, and bond distances N1-H and N2---H1W of 0.84 and 2.26 Å respectively. *E*-DPYDPE didn't show any inter or intramolecular H-bonding, which may be because of long distances between the NH groups of nearby molecules. The dissimilarities in molecular shapes and structural polarities of *E*- and *Z*-isomers, due to the presence of intramolecular H-bonding in *Z*-isomer, assisted in easier separation of *E*- and *Z*-isomers by fractional crystallization technique.

E- and *Z*-isomer of DPYDPE were further characterized by using ^{1}H NMR and ^{1}H- ^{1}H COSY NMR spectroscopy (Figure S5 and S6 in ESI). The comparison of the ^{1}H NMR spectra of *E*- and *Z*- isomers along with *E/Z* mixture is shown in **Figure 2**. It can be seen that in both *E*- and *Z*-isomers, all the phenylic protons are magnetically equivalent and resonates at 7.50 and 7.10 ppm respectively. The β–pyrrolic protons appeared at 6.18 and 5.96 ppm for *Z*-isomer, whereas at 5.95 and 5.38 ppm for *E*-isomer. In *E*-isomer, pyrrole α–H and NH resonates at 6.45 and 7.23 ppm, whereas respective protons resonate for *Z*-isomer at 6.70 and 8.08 ppm. Intramolecular H-bonding between the pyrrolic NH lead to downfield shift in all the pyrrolic protons and upfield shift in phenylic protons in Z-isomer compared to E-isomer. The *E*-and *Z* -ratio of the isomers in the *E/Z* mixture was determined as 5:4 by integration of pyrrole α–H protons in ^{1}H NMR.

2.3. Photophysical properties of E- and Z-isomers of DPYDPE

After confirming the structures of *E*- and *Z*-DPYDPE isomers, we have investigated their photophysical properties. The comparison of normalized absorption and fluorescence spectra are shown in **Figure 3(a)** and **3(b)** respectively. *E*-DPYDPE showed absorption peak at 357 nm, emission at 461 nm in THF (λ_{ex}=350 nm), whereas *Z*-DPYDPE showed absorption at 340 nm and emission at 470 nm in THF. *E*-DPYDPE is less fluorescent similar to TPE with quantum yield of 0.23%, whereas *Z*-DPYDPE was significantly fluorescent with quantum yield of 6%. To test the possibility of *EZ*I in pure *E*- or *Z*-isomer under present experimental conditions, we have kept chloroform-d solution of pure *E*- and *Z*-isomers of DPYDPE separately in continuous radiation under xenon lamp for 40 min at λ_{ex}=350 nm. The ^{1}H NMR spectra of both showed no spectral change, indicating *EZ*I process has not occurred.

2.4. AIE vs CIE

By inspecting the structure of the *E*- and *Z*-DPYDPE molecules, we can see that pyrrole rings and phenyl rings are free to move around vinyl stator. This property makes these molecules to behave as AIE gens. To confirm this, we have studied photoluminescence behaviors of both compounds using THF/water mixtures with different fractions of water. Both these isomers showed AIE in THF/Water due to the formation of aggregates. E-isomer was weakly emissive in THF solution and showed strong emission from f_w 70-85% due to aggregate formation, followed by reduced emission due to agglomeration (**Figure 4(a)**). Whereas *Z*-DPYDPE, which was fairly emissive in THF showed decrease in emission till f_w=80% and then sudden increase from f_w 80-90% due to aggregation and again decreased to 95% because of agglomeration (**Figure 4(b)**). The comparison of PL of *E*- and *Z*-DPYDPE along with TPE at f_w = 90% shown in **Figure 4 (c)**. The quantum yield measurement showed that E isomer posses better AIE behavior with quantum yield of 69% than both *Z*- isomer (Φ = 37%) and TPE (Φ = 14.0%) (**Table 2**). This gives a high $\alpha_{AIE}= \Phi_{agg}/ \Phi_{sol}$ value of 299 for *E*-DPYDPE

and 6 for *Z*-DPYDPE. Thus, *E*-DPYDPE is better AIEgen than *Z*-DPYDPE. In **Figure 4 (d)**, a comparative AIE behavior of *E*- and *Z*-DPYDPE along with TPE is shown. It can be seen that *E*-isomer is forming aggregates at lower f_w of 70% than *Z*-isomer, which indicates that *Z*-isomer is more polar than E-isomer. Fluorescence decay lifetime of *E*- and *Z*- isomers measured at λ_{ex}=340 nm are 2.16 and 2.41 ns respectively (**Table 2**).

Both the *E*-and *Z*-isomers were fluorescent in solid state and fluorescent crystal images by confocal microscopy are shown in **Figure 5 (a) and 5 (b)**. Solid-state PL spectra were recorded by making films on quartz substrate and the solid films were found to be crystalline by XRD. The PL maxima for films appeared at 483 and 489 nm for *E*- and *Z*-isomers respectively (**Figure 5(c)**). Unlike aggregates, in solid state, the *Z*-DPYDPE showed high fluorescence quantum yield of 89% as compared to *E*-DPYDPE (Φ = 10%) (**Figure 5(c)**). This indicates that *Z*- isomer is better CIEgen than *E*-isomer.[16,30] The difference in the behaviors of *E*- and *Z*- isomers can be explained by RIR mechanism, which is related to molecular packing as discussed in later section.

TEM and SEM imaging

From TEM and SEM imaging of f_w 90% aggregate solution, it can be seen that both the *E*- and *Z*-isomers of DPYDPE form microstructures (**Figure 6**). In *E*-DPYDPE, formation of long fibre like structures of length ~10-15 μm and width ~ 0.3 μm can be seen, whereas *Z*-DPYDPE exists in the form of bundles of small rods of length ~2-5 μm and width ~ 0.25 μm. Both the microstructures formed were amorphous in nature as predicted by specific area diffraction from TEM (**Figure 6(a)** and **(b)** inset) and powder XRD. The amorphous aggregates of *Z*-isomer were poorly emissive and of *E*-isomers were efficiently emissive. Since *E*-isomers are photoluminogens in aggregate phase, hence designated, as AIEgens and the *Z*-isomers are photoluminogens in crystalline phase, hence designated as CIEgens.

Molecular packing

Molecular packing of the *E*- and *Z*-DPYDPE molecules is shown in **Figure 7**. The analysis showed that, in *E*-isomer (**Figure 7(a)**), no apparent π–π stacking could be seen but eight weak CH–π interactions of 3.16 and 3.31 Å observed in *z* direction. This lead to formation of ladder like structures, packed in *xy* plane *via* weak van der Waals interactions. Such interactions could assist in locking the molecular motion in the crystal lattice and reducing the non-radiative deactivation of excitons.[53] Consequently, the loose packing mode and propeller-like structures will be beneficial for the photoluminescence in solid state.

In case of *Z*-isomer, no π–π interaction can be seen but strong intermolecular NH–π interaction of 3.3 Å and CH–π interactions of 3.5 and 2.9 Å, which lead to compact packing (**Figure 7 (b)**). Moreover intramolecular H-bonding between N_1–H_1w–N_2, NH–π interaction of 3.02 Å and CH–π interaction of 3.26 Å lead to restriction of intramolecular rotation and consequently the molecule showed efficient CIE behavior. Furthermore, molecular densities in crystal also indicate that *Z*-isomers (400 $Å^3$/molecule) were tightly packed than E-isomers (410 $Å^3$/molecule). Hence *Z*-isomers showed efficient CIE behavior than *E*-isomers.

In THF/Water mixtures, the intermolecular H-bonding interactions of Z-isomer with water overrules intramolecular H-bond and NH–π interactions, leading to formation of amorphous aggregates (*vide infra*), with less restricted rotations and hence favored radiationless decay, result in weak AIE. On the other hand, CH–π interactions between *E*-DPYDPE remain unaffected by water molecules in THF/Water mixtures, hence favored AIE. Therefore, we can say that molecular orientations and RIR play a key role to dictate the AIE and CIE behavior of *E*- and *Z*-isomers of DPYDPE.

Metal sensing behaviour

Since *E/Z*-DPYDPE compounds has two donor nitrogen atoms, we carried out preliminary metal sensing behaviour of *Z*-DPYDPE for sensing various metal ions such as Zn^{2+}, Cu^{2+},

Fe^{2+}, Hg^{2+}, Ni^{2+}, Co^{2+}, Cd^{2+} and Mn^{2+} in CH_3CN solvent. We carried out qualitative absorption and fluorescence studies of *Z*-DPYDPE in the presence of various metal ions in CH_3CN as shown in the Figure 8a/8b. Our studies clearly indicated that only in the presence of Hg(II) ion, there is a significant changes in the absorption and fluorescence properties of *Z*-DPYDPE indicating that *Z*-DPYDPE can be used as specific selective sensor for Hg(II) ion.

We also systematically carried out the absorption and fluorescence spectral titration of *Z*-DPYDPE upon addition of increasing amounts of Hg(II) ions in CH_3CN solution as shown in Figure 8c/8d. Upon addition of increasing amounts of Hg(II) ions to acetonitrile solution of *Z*-DPYDPE resulted in the significant decrease in the intensity of absorption band at 350 nm with concomittent appearense of new absorption bands at 312 and 395 nm with gradual increase in the intensity and two clear isosbestic points at 330 and 365 nm supporting the neat interconversion between the unbound and mercury bound complex (Figure 8c). In addition, we also noted the appearence of new absorption band at 680 nm upon gradual addition of Hg(II) ions, which could be tentatively attributed to the charge transfer band.

Similarly, the selective sensing of Hg(II) ion by *Z*-DPYDPE was also followed systematically by fluorescence titration experiments. The *Z*-DPYDPE is very weak fluorescent (λ_{max} = 445 nm) in solution with a quantum yield (Φ) of ~ 0.005. However, upon addition of three equivalents of Hg(II) ion, the fluorescence maxima of *Z*-DPYDPE at 445 nm experienced ~25 nm bathochromic shift (λ_{max} = 470 nm) with remarkable enhancement (68 fold) in the fluorescence intensity (Figure 8d). The significant enhancement in the fluorescent intensity of *Z*-DPYDPE accompanied by a clear colour change from non-fluorescent faded yellow to strongly fluorescent bluish green solution (Figure S11 in ESI) supports the mercury bound complex of *Z*-DPYDPE. We also carried out anion sensing behaviour of *Z*-DPYDPE with various anions. The compound *Z*-DPYDPE did not show any significant changes in the

absorption and emission spectra indicating that it didn't sense anions. Thus, our preliminary studies indicated that *Z*-DPYDPE selectively and specifically sense Hg(II) ion over other cations/anions. Detailed studies are underway and will be published in due course of time.

3. Conclusions

In conclusion, *E*- and *Z*-isomers of dipyrrolyldiphenylethene, which are similar to TPE, were synthesized by using traditional McMurry coupling. *E* and *Z* isomers of DPYDPE were separated, using easy crystallization technique by taking advantage of structural polarity difference due to intramolecular H-bonding in *Z*-DPYDPE. Their stereo structures were verified by spectroscopic techniques and crystallographic analysis. The *E*-isomer showed a pronounced AIE behaviour with α_{AIE}= 299 and Φ_{agg}= 69%, whereas *Z*-isomer showed CIE behaviour with Φ_{film}=89%. Under normal PL spectral conditions, no *EZ*I process was observed, which indicates that RIR is the main cause for AIE/CIE behaviour in DPYDPE luminogens. Thus, the pure isomers have permitted to examine the structure-morphology-function relationships, the effect of intramolecular H-bonding and NH–π interactions on molecular packing and crystallisation/aggregation induced emission. The preliminary sensing studies carried out with *Z*-DPYDPE indicated that it shows specific sensing for Hg^{2+} ion over other ions and the detail studies are underway in our laboratory.

4. Experimental Section

Experimental:

All the chemicals used for the synthesis were reagent grade unless otherwise specified. Column chromatography was performed on neutral alumina. The ^{1}H and ^{13}CNMR spectra were recorded in $CDCl_3$ on Bruker 400 and 500 MHz instrument using tetramethylsilane ($Si(CH_3)_4$) as internal standard. Absorption and steady state fluorescence spectra were obtained with Varian-Cary 100 Bio UV-Visible spectrophotometer and Varian-Cary Eclipse spectrofluorometer respectively. Solid-state absorption is measured on shimadzu UV 3600,

clubbed with integrating sphere. The fluorescence quantum yields (Φ) were estimated from the emission and absorption spectra by comparative method at the excitation wavelength of 340 nm using diphenyl anthracene in cyclohexane as standard, Φ_f = 97%[54] for solution and aggregates and Φ_f = 68%[54] for film. A picosecond pulsed diode laser based time correlated single photon counting (TCSPC) instrument from IBH (United Kingdom) is used to collect time-resolved decays at different wavelengths, with the emission polarizer set at a magic angle of 54.7° with respect to the polarization of the incident light. Pulsed laser sources of 340 nm with 250 ps fwhm are used having a resolution of 14ps/channel. The decay traces are fitted to a sum of exponential functions, as shown below using the iterative reconvolution technique by IBH DAS 6.2 data analysis software.[5556]

$$I(\lambda, t) = I_0(\lambda)\sum a_i e^{-t/\tau_i} \quad (1)$$

Here I(λ, t) is the fluorescence intensity at an emission wavelength of λ at a time t after excitation. $I_0(\lambda)$ is the fluorescence intensity at an emission wavelength of λ at time zero. τ_i and a_i are the lifetime and amplitude of the i^{th} component, respectively. The LR-MS spectra were recorded with a Q-Tof micro mass spectrometer.

Synthesis

1,2-Diphenyl dipyrroethene (DPYPDE)

An activated zinc powder (1.55 g, 24.2 mmol) in THF (40 mL) was taken in a three-necked round bottom flask and purged with nitrogen gas for 10 min. The mixture was cooled to 0°C and $TiCl_4$ (2.24 g, 11.9 mmol) was added slowly by maintaining the temperature at 0°C. The suspension was then warmed to room temperature and stirred for 30 min., followed by reflux for 3 h. The mixture was once again cooled to 0 °C, and the solution of 2-benzoyl pyrrole (0.45 g, 2.6 mmol) in THF (25 mL) was added slowly. The reaction mixture was refluxed for 12 h, until the starting material was completely consumed as monitored by TLC analysis. The reaction mixture was quenched with 10% aqueous NH_4Cl solution and extracted

with ether. The organic layers were collected, dried over anhydrous Na_2SO_4 and concentrated on rotary evaporator under vacuum. The crude compound was purified by column chromatography on neutral alumina using (9:1 v/v) petroleum ether/ ethyl acetate and afforded desired *E/Z* mixture 1,2-diphenyldipyrroethene as pale colourless solid in 52% yield (0.20 g). ^{1}H NMR (400 MHz, Chloroform-d_3, δ in ppm): 8.08 (2 H_z, bs), 7.57 - 7.40 (10 H_E, m), 7.23 (2 H_E, bs), 7.11 - 7.08 (10 H_z, m), 6.71 - 6.70 (2 H_z, m), 6.45 - 6.43 (2 H_E, m), 6.18 - 6.17 (2 H_z, m), 6.00 - 5.91 (4 $H_{E/Z}$, m), 5.40 - 5.38 ppm (2 H_E, m); *E/Z* ratio= 5:4; MS (2000 eV): *m*/*z* (%): 309 (100) [M-H^+]

E/Z isomers were separated by crystallisation in CH_2Cl_2/ hexane. After complete crystallisation, mother liquor was removed and crystals were washed with CH_2Cl_2 once. Yellow triclinic crystals (*Z*-isomer) remain undissolved and White needle like crystals (*E*-isomer) were dissolved completely. CH_2Cl_2 solution was evaporated to dryness and again kept for crystallisation in CH_2Cl_2/ hexane. After partial crystallisation, pure *E*-isomer was collected. Mother liquor was evaporated, kept for crystallisation and process is repeated from the second step *i.e.* washing with CH_2Cl_2. Pure *E* and *Z* isomers are characterised by ^{1}H NMR and ^{13}C NMR.

E-DPYDPE: M. P. decomposes at 200^{o}C; ^{1}H NMR (400 MHz, Chloroform- d_3, δ in ppm): 7.55 - 7.43 (10 H, m), 7.23 (2 H, bs), 6.45 - 6.43 (2 H, m), 5.96 - 5.94 (2 H, m), 5.40 - 5.38 (2 H, m); ^{13}C NMR (101 MHz, $CDCl_3$, δ in ppm): 108.62, 118.80, 128.12, 129.41, 130.88, 133.48, 141.67. λ_{max} (ε)=357 nm (1000 $mol^{-1}dm^3cm^{-1}$)

Z-DPYDPE: M. P. decomposes at 200^{o}C; ^{1}H NMR (500 MHz, Chloroform- d_3, δ in ppm): 8.08 (2 H, bs), 7.11 - 7.08 (10 H, m), 6.71- 6.70 (2 H, m), 6.18 - 6.17 (2 H, m), 5.97 - 5.95 (2 H, m); ^{13}C NMR (101 MHz, $CDCl_3$, δ in ppm): 108.62, 118.80, 128.12, 129.41, 130.88, 133.48, 141.67. λ_{max} (ε)=340 nm (456 $mol^{-1}dm^3cm^{-1}$)

Preparation of Nano aggregates

A stock solution of *E*- or *Z*-DPYDYE in THF with a concentration of 1 mM was prepared. Aliquots (1 mL) of the stock solution were transferred to 10 mL volumetric flasks. After adding appropriate amounts of THF, water was added dropwise under vigorous stirring to furnish 0.1 μM solutions with defined fractions of water (f_w = 0–95 vol %). These fractions were further diluted to get 10μM concentrations by adding desired THF/Water mixtures. Spectral measurements of the solutions or suspensions were performed immediately.

Preparation of samples for SEM and TEM studies

Samples were made by dropcasting f_w=90% solutions of *E*- and *Z*-DPYDYE on desired substrate (*E*-DPYDPE on carbon paint and *Z*-DPYDPE on silicon wafer) and solvent was dried at room temperature followed by annealing at 100^{o}C for 15 minutes. Before SEM samples were sputter coated with platinum metal to avoid charging.

Single crystal studies

High-quality single crystals of DPYDPE were grown from a DCM/ hexane mixture at room temperature. A suitable crystal of size 0.03 x 0.06 x 0.40 mm^3 (*E*-DPYDPE) and 0.03 x 0.06 x 0.38 mm^3 (*Z*-DPYDPE) was mounted on a Rigaku Saturn 724+ CCD diffractometer for unit cell determination and three dimensional intensity data collection. 800 frames in total were collected at 150 K with the exposure time of 28 s per frame. Data integration, indexing and absorption correction using Crystal clear followed by structure solution using the programs in WinGX module.[57] The structure was solved by direct method (SIR-92) and the final refinement of the structure was carried out using full least-squares methods on F^2 using SHELXL-97.[58,59] Unit cell determination using both high and low angle reflections reveal that compound *E*-DPYDPE and *Z*-DPYDPE crystallizes in tetragonal I 41/a and triclinic P-1 space group respectively. Non-hydrogen atoms were refined anisotropically. C–H hydrogen atoms were placed in geometrically calculated positions by using a riding model. The final

refinement of the solved structure yielded the final R-value of 0.1000 (*E*-DPYDPE) and 0.0876 (*Z*-DPYDPE) (I>2σ(I))

[CCDC 1051020 and1051021 contains the supplementary crystallographic data for this paper. These data can be obtained free of charge from The Cambridge Crystallographic Data Centre via www.ccdc.cam.ac.uk/data_request/cif.]

[Further details of the crystal structure investigation(s) may be obtained from the Fachinformationszentrum Karlsruhe, 76344 Eggenstein-Leopoldshafen (Germany), on quoting the depository number CSD1051020 and1051021.]

Corresponding Author

*Email: ravikanth@chem.iitb.ac.in

ACKNOWLEDGMENT

KG and MR acknowledges Department of Science and Technology for funding (CS-367/2013) and Indian Institute of Technology Bombay, Mumbai for providing infrastructure for the accomplishment of the project. The authors thank Prof. R. Murugavel for allowing us to use the single crystal X-ray diffraction facility established through a DAE-SRC outstanding investigator award.

References

1 H. Li, Z. Chi, X. Zhang, B. Xu, S. Liu, Y. Zhang and J. Xu, *Chem. Commun.*, 2011, **47**, 11273–11275.

2 J. Huang, X. Yang, X. Li, P. Chen, R. Tang, F. Li, P. Lu, Y. Ma, L. Wang, J. Qin, Q. Li and Z. Li, *Chem. Commun.*, 2012, **48**, 9586.

3 J. Huang, X. Yang, J. Wang, C. Zhong, L. Wang, J. Qin and Z. Li, *J. Mater. Chem.*, 2012, **22**, 2478–2484.

4 Y. Hong, J. W. Y. Lam and B. Z. Tang, *Chem. Commun.*, 2009, 4332–4353.

5 M. Wang, G. Zhang, D. Zhang, D. Zhu and B. Z. Tang, *J. Mater. Chem.*, 2010, **20**, 1858–1867.

6 Z. Zhao, S. Chen, X. Shen, F. Mahtab, Y. Yu, P. Lu, J. W. Y. Lam, H. S. Kwok and B. Z. Tang, *Chem. Commun.*, 2010, **46**, 686–688.

7 J. Wang, J. Mei, R. Hu, J. Z. Sun, A. Qin and B. Z. Tang, *J. Am. Chem. Soc.*, 2012, **134**, 9956–9966.

8 H. Tong, Y. Dong, Y. Hong, M. Häussler, J. W. Y. Lam, H. H.-Y. Sung, X. Yu, J. Sun, I. D. Williams, H. S. Kwok and B. Z. Tang, *J. Phys. Chem. C*, 2007, **111**, 2287–2294.

9 N. B. Shustova, B. D. McCarthy and M. Dincă, *J. Am. Chem. Soc.*, 2011, **133**, 20126–20129.

10 J. Liu, J. W. Y. Lam and B. Z. Tang, *Chem. Rev.*, 2009, **109**, 5799–5867.

11 A. C. Grimsdale, K. Leok Chan, R. E. Martin, P. G. Jokisz and A. B. Holmes, *Chem. Rev.*, 2009, **109**, 897–1091.

12 M. Shimizu, H. Tatsumi, K. Mochida, K. Shimono and T. Hiyama, *Chem. – An Asian J.*, 2009, **4**, 1289–1297.

13 A. Iida and S. Yamaguchi, *Chem. Commun.*, 2009, 3002–3004.

14 A. Loudet and K. Burgess, *Chem. Rev.*, 2007, **107**, 4891–4932.

15 J. Luo, Z. Xie, J. W. Y. Lam, L. Cheng, H. Chen, C. Qiu, H. S. Kwok, X. Zhan, Y. Liu, D. Zhu and B. Z. Tang, *Chem. Commun.*, 2001, 1740–1741.

16 Y. Dong, J. W. Y. Lam, A. Qin, J. Sun, J. Liu, Z. Li, J. Sun, H. H. Y. Sung, I. D. Williams, H. S. Kwok and B. Z. Tang, *Chem. Commun. (Camb).*, 2007, 3255–3257.

17 Z. Zhao, J. W. Y. Lam and B. Zhong Tang, *Curr. Org. Chem.*, 2010, 14, 2109–2132.

18 I. Javed, T. Zhou, F. Muhammad, J. Guo, H. Zhang and Y. Wang, *Langmuir*, 2012, **28**, 1439–1446.

19 Z. Li, Y. P. Y. Q. Dong, J. W. Y. Lam, J. Sun, A. Qin, M. Häußler, Y. P. Y. Q. Dong, H. H. Y. Sung, I. D. Williams, H. S. Kwok and B. Z. Tang, *Adv. Funct. Mater.*, 2009, **19**, 905–917.

20 W. Z. Yuan, Y. Tan, Y. Gong, P. Lu, J. W. Y. Lam, X. Y. Shen, C. Feng, H. H.-Y. Y. Sung, Y. Lu, I. D. Williams, J. Z. Sun, Y. Zhang and B. Z. Tang, *Adv. Mater.*, 2013, **25**, 2837–2843.

21 S.-L. Deng, T.-L. Chen, W.-L. Chien and J.-L. Hong, *J. Mater. Chem. C*, 2014, **2**, 651–659.

22 G. Liang, J. W. Y. Lam, W. Qin, J. Li, N. Xie and B. Z. Tang, *Chem. Commun.*, 2014, **50**, 1725–1727.

23 G. Zhang, Z.-Q. Chen, M. P. Aldred, Z. Hu, T. Chen, Z. Huang, X. Meng and M.-Q. Zhu, *Chem. Commun.*, 2014, **50**, 12058–12060.

24 C. Zhang, S. Jin, K. Yang, X. Xue, Z. Li, Y. Jiang, W.-Q. Chen, L. Dai, G. Zou and X.-J. Liang, *ACS Appl. Mater. Interfaces*, 2014, **6**, 8971–8975.

25 D. Chen, X. Feng, S. Gu, B. Tong, J. Shi, J. Zhi and Y. Dong, *Chinese Sci. Bull.*, 2013, **58**, 2728–2732.

26 Q. Wu, Q. Peng, Y. Niu, X. Gao and Z. Shuai, *J. Phys. Chem. A*, 2012, **116**, 3881–3888.

27 Z. Zhao, P. Lu, J. W. Y. Lam, Z. Wang, C. Y. K. Chan, H. H. Y. Sung, I. D. Williams, Y. Ma and B. Z. Tang, *Chem. Sci.*, 2011, **2**, 672–675.

28 J. Chen, C. C. W. Law, J. W. Y. Lam, Y. Dong, S. M. F. Lo, I. D. Williams, D. Zhu and B. Z. Tang, *Chem. Mater.*, 2003, **15**, 1535–1546.

29 Z. Zhao, Z. Chang, B. He, B. Chen, C. Deng, P. Lu, H. Qiu and B. Z. Tang, *Chem. - A Eur. J.*, 2013, **19**, 11512–11517.

30 Y. Dong, J. W. Y. Lam, A. Qin, Z. Li, J. Sun, H. H.-Y. Sung, I. D. Williams and B. Z. Tang, *Chem. Commun. (Camb).*, 2007, **1**, 40–42.

31 C. Yang, Q. T. Trinh, X. Wang, Y. Tang, K. Wang, S. Huang, X. Chen, S. H. Mushrif and M. Wang, *Chem. Commun.*, 2015, **51**, 3375–3378.

32 B.-K. An, S.-K. Kwon, S.-D. Jung and S. Y. Park, *J. Am. Chem. Soc.*, 2002, **124**, 14410–14415.

33 J. Mei, Y. Hong, J. W. Y. Lam, A. Qin, Y. Tang and B. Z. Tang, *Adv. Mater.*, 2014, **26**, 5429–79.

34 A. Qin, J. W. Y. Lam, L. Tang, C. K. W. Jim, H. Zhao, J. Sun and B. Z. Tang, *Macromolecules*, 2009, **42**, 1421–1424.

35 Y. Dong, J. W. Y. Lam, A. Qin, J. Liu, Z. Li, B. Z. Tang, J. Sun and H. S. Kwok, *Appl. Phys. Lett.*, 2007, **91**, 2007–2009.

36 Y. Jiang, Y. Wang, J. Hua, J. Tang, B. Li, S. Qian and H. Tian, *Chem. Commun.*, 2010, **46**, 4689–4691.

37 C. L. Schilling and E. F. Hilinski, *J. Am. Chem. Soc.*, 1988, **110**, 2296–2298.

38 D. A. Shultz and M. A. Fox, *J. Am. Chem. Soc.*, 1989, **111**, 6311–6320.

39 A. Simeonov, M. Matsushita, E. A. Juban, E. H. Z. Thompson, T. Z. Hoffman, A. E. B. Iv, M. J. Taylor, P. Wirsching, W. Rettig, J. K. Mccusker, R. C. Stevens, D. P. Millar, P. G. Schultz, R. A. Lerner and K. D. Janda, 2000, **290**, 307–314.

40 D. H. Waldeck, *J. Mol. Liq.*, 1993, **57**, 127–148.

41 N. York, 1993, 10791–10795.

42 J. Bao and P. M. Weber, *J. Am. Chem. Soc.*, 2011, **133**, 4164–4167.

43 E. W. Debler, G. F. Kaufmann, M. M. Meijler, A. Heine, J. M. Mee, G. Pljevaljc, A. J. Di Bilio, P. G. Schultz, D. P. Millar, K. D. Janda, I. A. Wilson, H. B. Gray and R. A. Lerner, 2008, **2172**, 1232–1236.

44 A. Baldridge, S. R. Samanta, N. Jayaraj, V. Ramamurthy and L. M. Tolbert, *J. Am. Chem. Soc.*, 2010, **132**, 1498–1499.

45 J. Dong, K. M. Solntsevn and L. M. Tolbert, *J. Am. Chem. Soc.*, 2009, **131**, 662–670.

46 Z. Zhao, Z. Wang, P. Lu, C. Y. K. Chan, D. Liu, J. W. Y. Lam, H. H. Y. Sung, I. D. Williams, Y. Ma and B. Z. Tang, *Angew. Chemie Int. Ed.*, 2009, **48**, 7608–7611.

47 Q. Peng, Y. Yi, Z. Shuai and J. Shao, *J. Am. Chem. Soc.*, 2007, **129**, 9333–9339.

48 K.-Y. Pu and B. Liu, *Adv. Funct. Mater.*, 2009, **19**, 277–284.

49 Y. You, H. S. Huh, K. S. Kim, S. W. Lee, D. Kim and S. Y. Park, *Chem. Commun.*, 2008, 3998–4000.

50 J. Wu, W. Liu, J. Ge, H. Zhang and P. Wang, *Chem. Soc. Rev.*, 2011, **40**, 3483–3495.

51 H. N. Kim, Z. Guo, W. Zhu, J. Yoon and H. Tian, *Chem. Soc. Rev.*, 2011, **40**, 79–93.

52 J. Chen and Y. Cao, *Macromol. Rapid Commun.*, 2007, **28**, 1714–1742.

53 C. Stubhan, Tobias and Ameri, Tayebeh and Salinas, Michael and Krantz, Johannes and Machui, Florian and Halik, Marcus and Brabec, T. Stubhan, T. Ameri, M. Salinas, J. Krantz, F. Machui, M. Halik and C. J. Brabec, *Appl. Phys. Lett.*, 2011, **98**, 101–104.

54 Y. Fujiwara, R. Ozawa, D. Onuma, K. Suzuki, K. Yoza and K. Kobayashi, *J. Org. Chem.*, 2013, **78**, 2206–2212.

55 T. K. Mukherjee, D. Panda and A. Datta, *J. Phys. Chem. B*, 2005, **109**, 18895–18901.

56 P. P. Mishra, A. L. Koner and A. Datta, *Chem. Phys. Lett.*, 2004, **400**, 128–132.

57 L. Farrugia, *J. Appl. Crystallogr.*, 1999, **32**, 837–838.

58 G. M. Sheldrick,University of Göttingen: Göttingen, Germany, 1997.

59 G. Sheldrick, *Acta Crystallogr. Sect. A*, 2008, **64**, 112–122.

Legends

Scheme 1. Synthesis of dipyrrolyldiphenylethene (**DPYDPE**)

Figure 1. Crystal structures of (a) *E*- and (b) *Z*-DPYDPE.

Figure 2. ^{1}H NMR of *E*, *Z* and mixture of *E*- and *Z*-DPYDPE recorded in $CDCl_3$.

Figure 3. (a) Normalized absorbance and (b) Fluorescence of 10 μM solution of *E*- and *Z*-DPYDPE in THF at λ_{ex}=350 nm.

Figure 4. (a) and (b) PL spectra of *E*-and *Z*-DPYDPE and in THF/Water mixtures with different water fractions respectively; λ_{ex}=350 nm at 10μM; inset: Optical images of 90% and 10% aggregate solution. (c) PL spectra of TPE, *E*- and *Z*-DPYDPE at 10μM; λ_{ex}=350 nm. (d) Variation in PL intensity of TPE, *E*- and *Z*-DPYDPE and in THF/Water mixtures with different water fractions

Figure 5. (a) and (b) single crystal images by fluorescence confocal microscopy. (Merged images white light and UV light) (c) PL of TPE, *E*- and *Z*-DPYDPE in thin films on quartz.

Figure 6. (a) and (b) FEG-TEM images of *E* -DPYDPE and *Z*-DPYDPE on porous copper grids; inset: crystalline diffraction pattern; (c) and (d) FEG-SEM images of *E*-DPYDPE on carbon paste and *Z*-DPYDPE on silicon (100) wafer.

Figure 7. (a) and (b) Molecular packing of *E*-and *Z*-DPYDPE in single crystal, weak interactions and distances are shown with green colour (NH−π, CH−π and intramolecular H-bonding).

Figure 8. Qualitative (a) absorption and (b) emission spectral changes of *Z*-DPYDPE (5 μM) upon addition of excess equivalents of various metal ions in CH_3CN solution. Quantitative (c) absorption and (d) emission spectral changes of *Z*-DPYDPE (5 μM) upon addition of increasing equivalents of Hg^{2+} ions (0-4.5 equivalents) in CH_3CN solution.

Table 1. X-crystallography details of E−DPYDPE and *Z*-DPYDPE

Table 2. Comparison of Quantum yields, lifetimes and their relative contributions of *E*-, *Z* -DPYDPE and TPE.

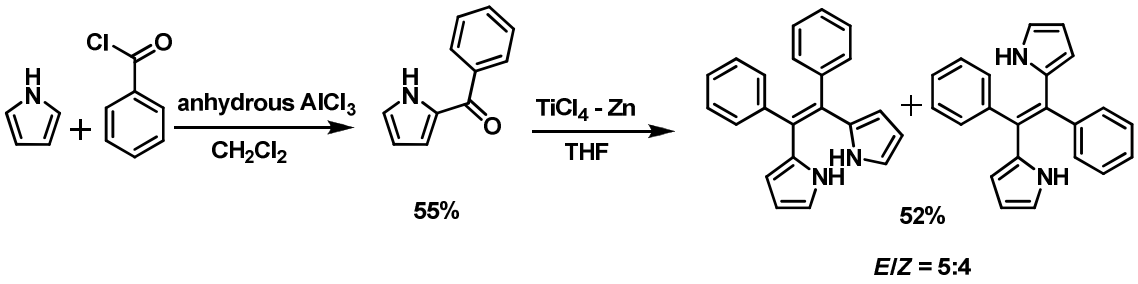

Scheme 1

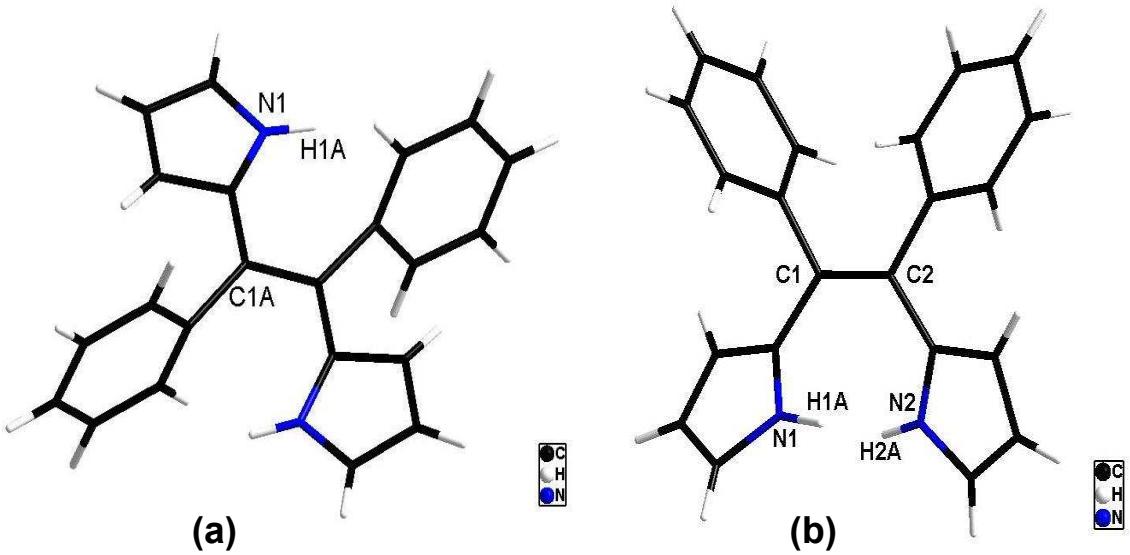

Figure 1

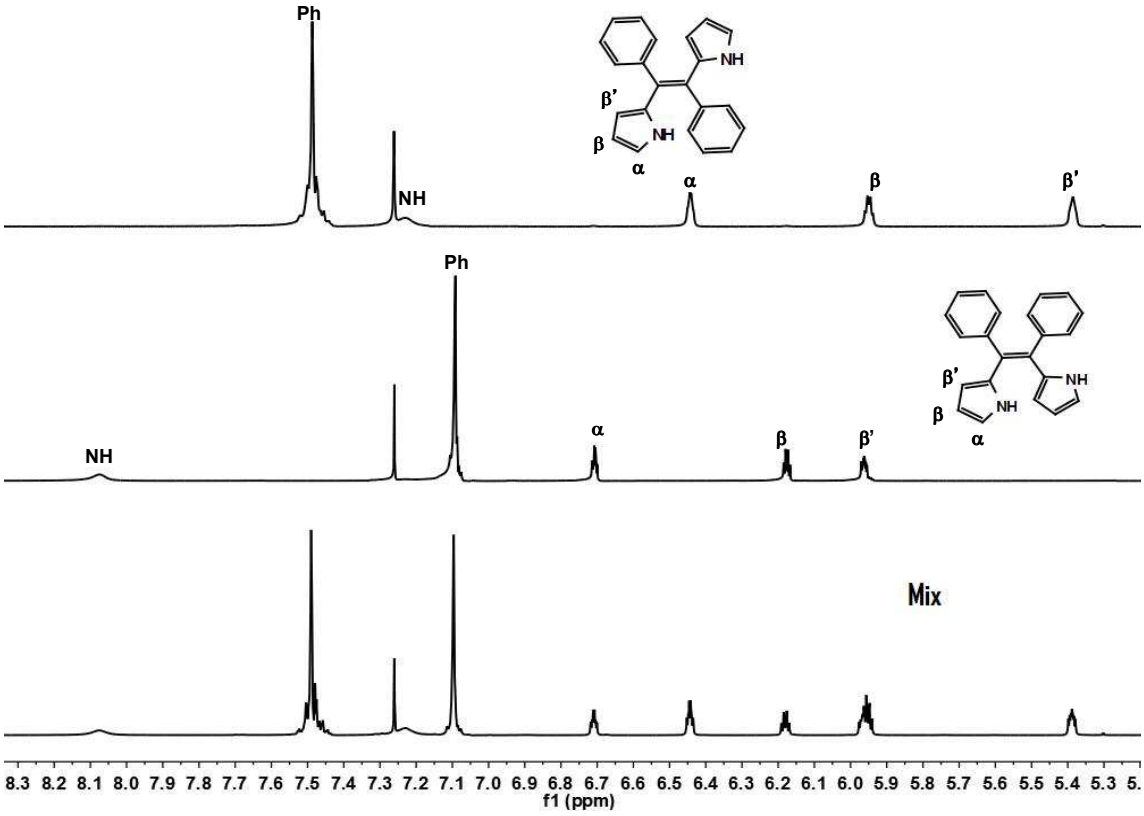

Figure 2

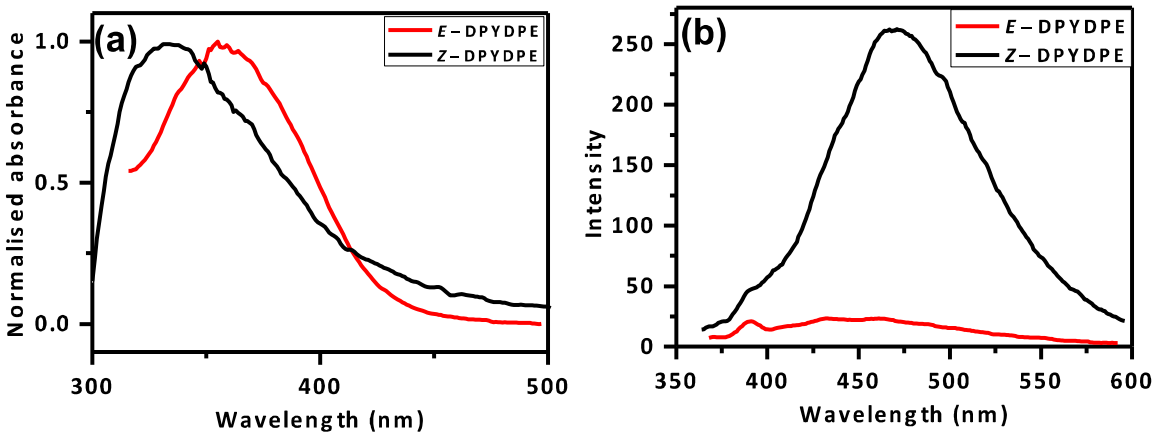

Figure 3

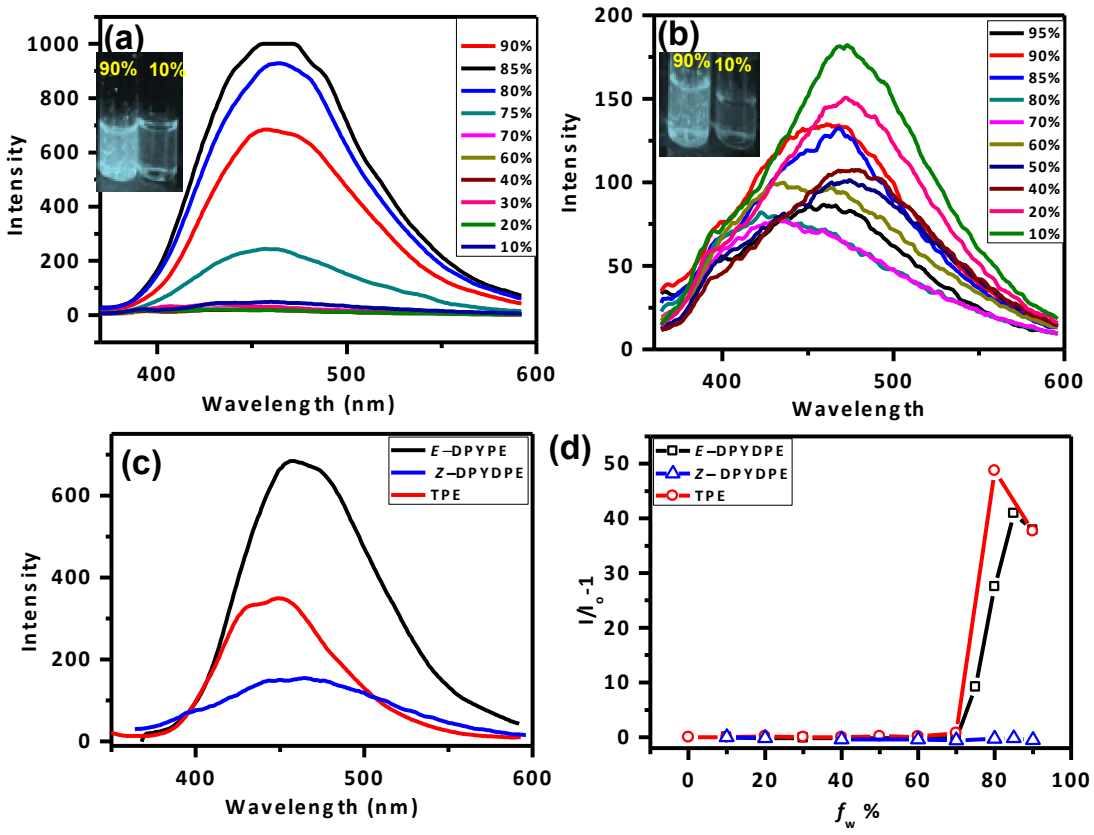

Figure 4

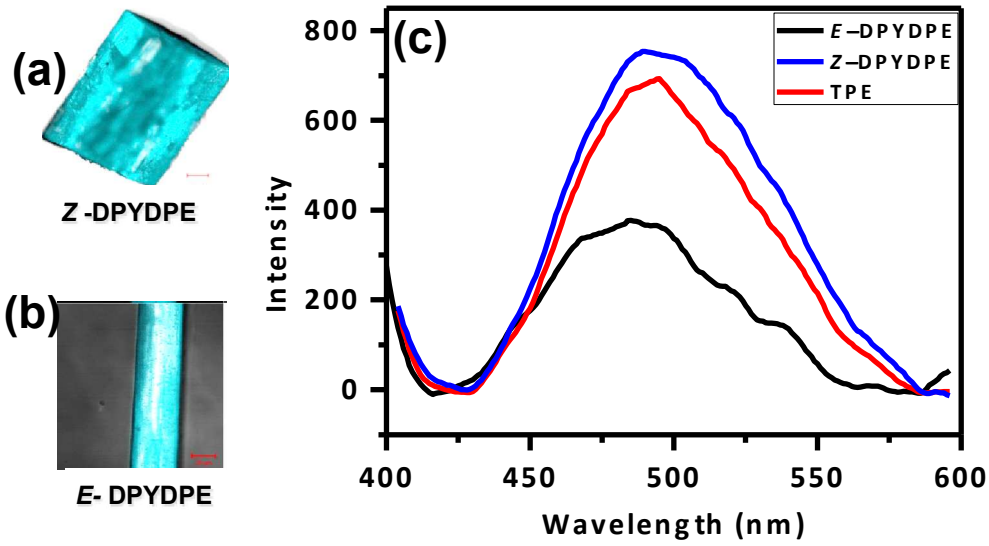

Figure 5

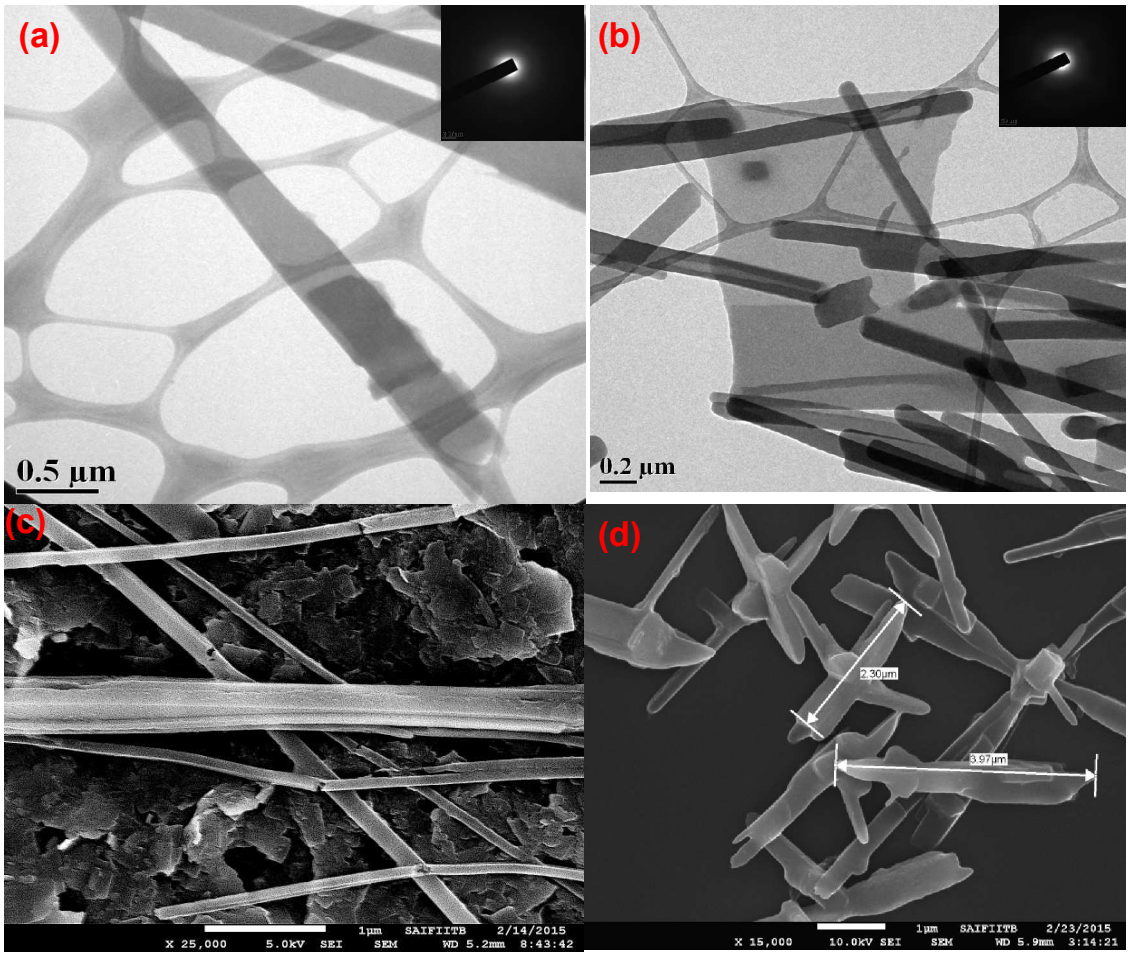

Figure 6

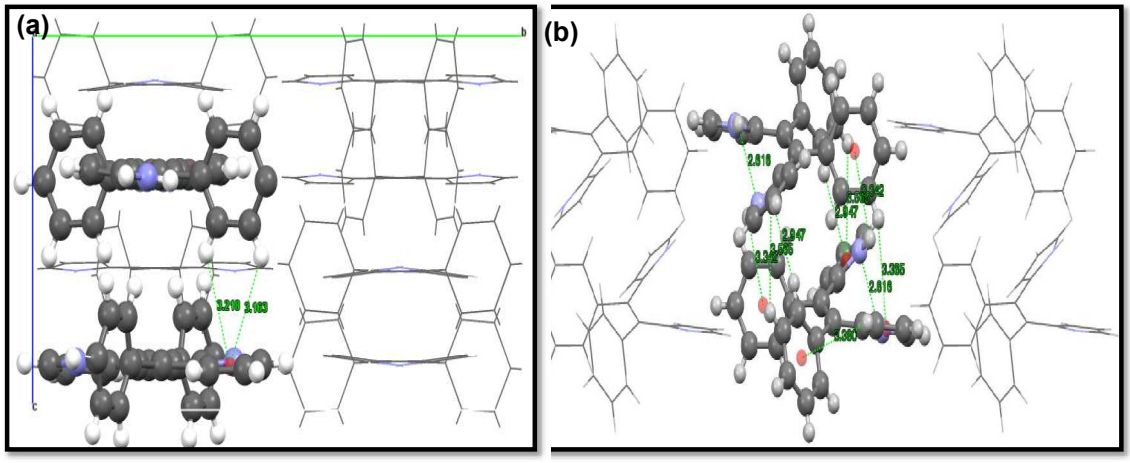

Figure 7

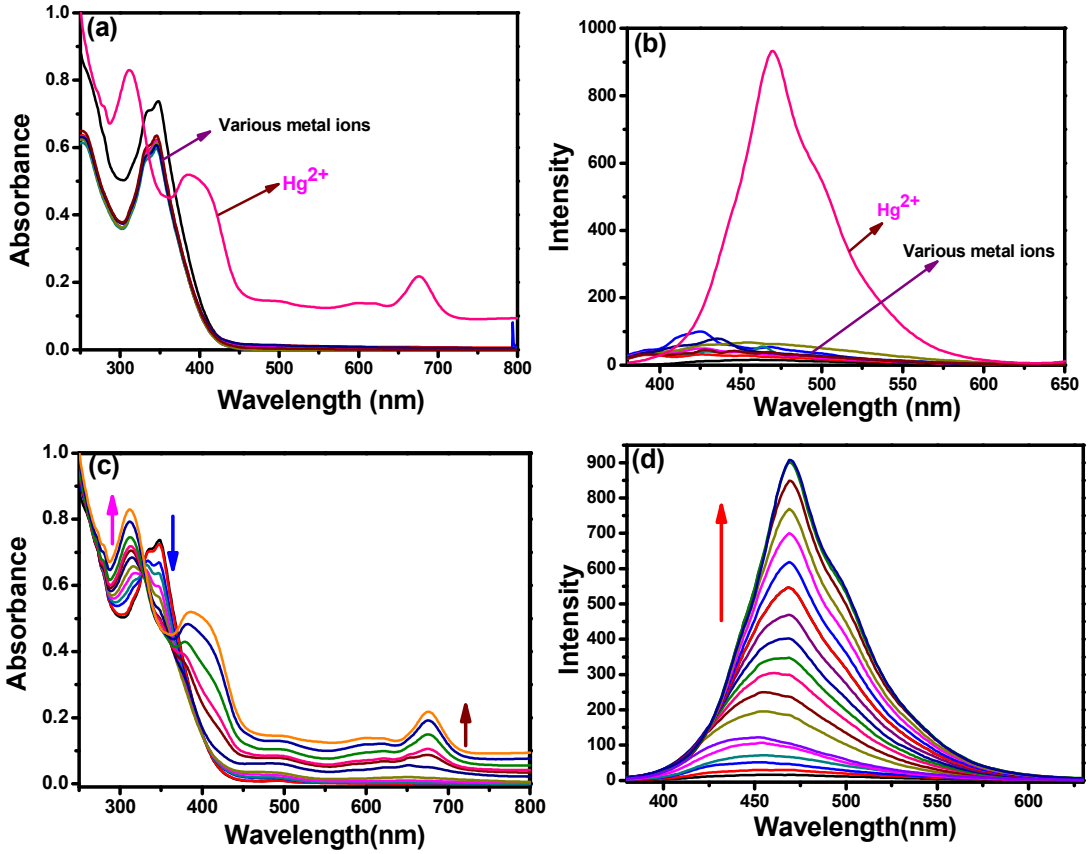

Figure 8

Table 1

Parameters	***E*-DPYDPE**	***Z*-DPYDPE**
Identification number	MR-KG-N1	MR-KG-N2
CCDC No	1051020	1051021
mol formula	$C_{22}H_{18}N_2$	$C_{22}H_{18}N_2$
fw	310.38	310.38
cryst sym	Tetragonal	Triclinic
Space group	I-41/a	P-1
a (Å)	18.225(9)	8.440(2)
b (Å)	18.225(9)	9.676(2)
c (Å)	9.896(5)	10.316(3)
α (deg)	90	75.506(9)
β (deg)	90	87.977(11)
γ (deg)	90	79.212(9)
V (Å^3)	3297(3) Å^3	801.2(3) Å^3
Z	8	2
μ (mm^{-1})	0.074	0.076
D_{calcd} (g cm^{-3})	1.254	1.287
F(000)	1312	328.0
θ range (deg)	1.58 - 25.11	1.58 - 25.11
Independent refections	6959 [R(int) = 0.0885]	6959 [R(int) = 0.0885]
R1, wR2 [$I > 2\sigma(I)$]	0.1000, 0.2249	0.1081, 0.2249
R1, wR2 (all data)	0.2010, 0.2662	0.2010, 0.2662
GOF	0.966	0.966
Largest diff. peak/hole, (e Å^{-3})	0.516, -0.599	0.516, -0.599

Table 2

Standard used is diphenylanthracene [a]: ϕ=97%[54] [b]: ϕ_{film}=68%[54]

	τ_1(ns)	A_1	τ_2(ns)	A_2	τ_m	Φ %	α_{AIE}
E-DPYDPE$_{agg}$	1.8	0.8	3.7	0.2	2.2	69[a]	299
E-DPYDPE$_{film}$	1.2	0.7	3.8	0.3	1.8	10[b]	-
E-DPYDPE$_{soln}$	nd	nd	nd	nd	nd	0.2[a]	-
Z-DPYDPE$_{soln}$	1.4	0.5	6.4	0.5	3.9	6 [a]	6
Z-DPYDPE$_{agg}$	1.3	0.6	4.3	0.4	2.4	37[a]	-
Z-DPYDPE$_{film}$	3.2	0.1	1.0	0.9	1.2	89[b]	-
TPE $_{agg}$	1.2	0.8	3.7	0.2	1.7	14[a]	56
TPE$_{Soln}$	nd	nd	nd	nd	nd	0.25[a]	-
TPE$_{film}$	1.6	0.6	4.3	0.3	2.5	48[b]	-

The table of contents entry

Aggregation/ Crystallization Induced Emission of *E*- and *Z*- Isomers of diphenyldipyrroethene have been demonstrated. We have successfully separated and characterized *E*- and *Z*-isomers of diphenyldipyrroethene molecules and studies show that E-isomer behaves as AIEgen, whereas Z-isomer as CIEgen.

Keyword
(Aggregation Induced Emission; Crystallization Induced Emission, Diphenyldipyrroethene, the *E/Z* Isomerization, Restriction of Intramolecular Rotation)

Dr. K. Garg, Mr. E. Ganapathi, Dr. P. Rajakannu, Prof. M. Ravikanth*

Stereochemical Modulation of Emission Behavior in *E/Z* Isomers of Diphenyldipyrroethene from Aggregation Induced Emission to Crystallization Induced Emission